Open access • Journal Article • DOI:10.1021/JP811201X

Anodic Formation of Ordered TiO2 Nanotube Arrays: Effects of Electrolyte Temperature and Anodization Potential — Source link

Jun Wang, Zhiqun Lin

Institutions: Iowa State University

Published on: 18 Feb 2009 - Journal of Physical Chemistry C (American Chemical Society)

Topics: Electrolyte and Indium tin oxide

THE JOURNAL OF PHYSICAL CHEMISTRY C

Article

Anodic Formation of Ordered TiO Nanotube Arrays: Effects of Electrolyte Temperature and Anodization Potential

Jun Wang, and Zhiqun Lin

J. Phys. Chem. C, **2009**, 113 (10), 4026-4030• DOI: 10.1021/jp811201x • Publication Date (Web): 18 February 2009

Anodic Formation of Ordered TiO_2 Nanotube Arrays: Effects of Electrolyte Temperature and Anodization Potential

Jun Wang and Zhiqun Lin*

Department of Materials Science and Engineering, Iowa State University, Ames, Iowa 50011

Received: December 18, 2008; Revised Manuscript Received: January 15, 2009

Highly ordered TiO_2 nanotube arrays were fabricated via electrochemical anodization of high purity Ti foil and Ti thin film coated indium tin oxide (ITO) glass in fluorine containing electrolytes (both aqueous and nonaqueous). The formation of ordered TiO_2 nanotube arrays was affected by the electrolyte temperature and the applied anodization potential. In aqueous electrolyte, the anodization potential exerted significant influence on the formation of TiO_2 nanotube arrays, while little effect from the electrolyte temperature was observed. In nonaqueous electrolyte, the electrolyte temperature markedly affected the TiO_2 nanotube dimensions, while the anodization potential exhibited slight influence in this regard. As a consequence, TiO_2 nanotube arrays with tube diameters ranging from 20 to 90 nm and film thicknesses ranging from several hundred nanometers to several micrometers were obtained. The TiO_2 nanostructures were examined by scanning electron microscopy. Thermal annealing on the anodized Ti induced crystalline formation, which was confirmed by Raman spectroscopy measurement.

Introduction

Since Zwilling and co-workers reported porous structure formation in Ti via electrochemical anodization in fluorine containing electrolytes in 1999,[1,2] tremendous research efforts have been made to fabricate TiO_2 nanostructures by anodization. Gong et al. were the first to demonstrate the fabrication of uniform TiO_2 nanotube arrays by electrochemically anodizing Ti in hydrofluoric acid aqueous solution.[3] In anodic TiO_2 nanotube arrays, each individual tube is perpendicular to the membrane surface, thereby providing larger surface areas and being an excellent module for use in optical and electronic devices (e.g., dye sensitized solar cells (DSSCs),[4−9] gas sensors,[10−12] hydrogen generators,[13,14] etc.). Recently, much work has been carried out on the synthesis and applications of ordered anodic TiO_2 nanotube arrays. Advance in synthetic techniques made it possible to prepare TiO_2 nanotube arrays with various pore diameters (10−110 nm), thicknesses (200 nm−1000 μm), and wall thicknesses (7−34 nm).[15−17] Fluorine containing electrolytes have been considered as the best electrolyte for anodic growth of TiO_2 nanotubes. In this context, three generations of electrolytes have been developed, that is, hydrofluoric acid aqueous solution,[3] fluorine containing buffer solution,[18] and nonaqueous electrolyte containing fluorine salt.[19,20] The formation of TiO_2 nanotube arrays is a direct consequence of competition between electrochemical oxidation of Ti and electrical field induced etching of TiO_2 as well as chemical etching of TiO_2 by fluorine ions.

It is noteworthy that TiO_2 has rather poor mechanical strength; thus, it is difficult to obtain the freestanding TiO_2 nanotube,[17,21] which, to some extent, limits its applications in certain fields where the nanotube arrays are required to be in intimate contact with other substrates. Recently, Mor and co-workers reported the fabrication of transparent TiO_2 nanotube arrays by anodizing Ti that was predeposited on a transparent substrate, and then successfully utilized the arrays for high performance DSSCs and hydrogen sensors.[6,11,22] We note that the thickness of the nanotubes was only on the order of several hundred nanometers due to the limited ability of depositing thicker high-quality Ti on the substrate;[6] it was suggested that the quality of the predeposited Ti film is key to producing highly ordered TiO_2 nanotube arrays.[6,22−24] The ability to grow TiO_2 nanotube arrays directly on substrates other than Ti foil not only shows the flexibility of electrochemical anodization process but also facilitates the extension of their promising applications. TiO_2 nanotubes obtained directly after anodization are amorphous and not photoactive; therefore, it is necessary to transform the amorphous TiO_2 nanotubes into crystalline form for a wide range of applications. High temperature annealing has been regarded as an effective route to inducing crystalline formation in as-prepared TiO_2 nanotube arrays, converting them into the anatase or rutile phase.[25] The annealed TiO_2 nanotube arrays retain their tubular morphology.[6,17]

Herein we report the study on electrochemical anodization of high purity Ti in both aqueous and nonaqueous electrolytes, with the main focus being on the effects of electrolyte temperature and anodization potential on the formation of TiO_2 nanotube arrays. The study showed that, in aqueous electrolyte (i.e., dilute hydrofluoric acid), formation of TiO_2 nanotube arrays was sensitive to the anodization potential, while in viscous nonaqueous electrolyte (i.e., glycerol) the electrolyte temperature was found to exert significant influence on the nanotube dimension. Both 0.25 mm thick Ti foil and 500 nm Ti coated indium tin oxide (ITO) glass were used for the growth of TiO_2 nanotube arrays. The as-prepared TiO_2 nanotube arrays were amorphous and converted into anatase phase via high temperature annealing; the crystalline transformation was confirmed by Raman spectroscopy measurement. To the best of our knowledge, this is the first report on the effect of electrolyte temperature on anodic formation of TiO_2 nanotube arrays.

Experimental Section

Chemicals. All chemicals were used as received without further purification. Ti foil (99.7% purity, 0.25 mm thick),

* To whom correspondence should be addressed. E-mail: zqlin@iastate.edu.

10.1021/jp811201x CCC: $40.75
Published on Web 02/18/2009

hydrofluoric acid (48 wt % in water), and ammonium fluoride (reagent, 98%) were purchased from Sigma-Aldrich. Acetic acid and glycerol were purchased from Fisher Scientific. Ti coated ITO glass was prepared by depositing 500 nm thick Ti using an e-beam evaporator. Before deposition, the ITO glass was cleaned by ultrasonicating in acetone, isopropyl alcohol, and methanol sequentially.

Anodization of Ti Foil. Ti foil was cut into 1×0.5 in.^{2} pieces. Before electrochemical anodization, Ti foil was degreased by ultrasonication in a mixture of acetone, methanol, and methylene chloride for 30 min, followed by washing with a large amount of DI water and drying with N_2. Electrochemical anodization was carried out in a two-electrode cell using a power source EC570-90 (Thermo Electron Corporation), where the Ti foil was used as the anode and a thin platinum foil was used as the counter electrode. Both aqueous electrolyte (i.e., 0.5 wt % hydrofluoric acid in DI water) and nonaqueous electrolyte (i.e., glycerol containing ammonium fluoride) were used. The anodization was performed either at room temperature (298 K) or in an ice bath. After a certain period of anodization (i.e., 4 h), the Ti foil was immediately washed with a large amount of DI water and subsequently dried with N_2. To induce the crystalline phase, the anodized Ti foil was annealed at 500 °C in air for 3 h.

Anodization of Ti Coated ITO Glass. Ti coated ITO glass (500 nm) was washed with acetone and isopropyl alcohol. Electrochemical anodization was performed in a two-electrode cell using a platinum foil as the counter electrode. Hydrofluoric acid aqueous solution (0.5 wt %, with acetic acid added in a volume ratio of 1:7) and glycerol solution containing 0.25 wt % ammonium fluoride were used as electrolytes. The anodization was stopped when the current dropped to zero, which was indicative of complete anodization of the Ti thin film. After anodization, the ITO glass was immediately washed with a large amount of DI water and dried with N_2. To induce crystalline phase, the anodized Ti coated ITO glass was annealed at 500 °C in air for 3 h.

Characterization. All anodized Ti (both Ti foil and Ti coated ITO glass) were characterized using a JEOL 5800 LV scanning electron microscope (SEM). The crystalline nature of both as-prepared and annealed TiO_2 nanotube arrays were examined using a Renishaw inVia Raman microscope equipped with an Ar laser (488 nm wavelength).

Results and Discussion

1. TiO_2 Nanotube Arrays Obtained from Aqueous Electrolyte. Fluorine containing electrolyte has been recognized as the most efficient electrolyte for anodic formation of TiO_2 nanotube arrays. In an electrochemical anodization process, TiO_2 nanotube arrays were formed via self-organization of TiO_2 as a result of the delicate balance of electrochemical oxidation of Ti into TiO_2, the electrical field induced dissolution of TiO_2, and the chemical dissolution of TiO_2 by fluorine ion. In aqueous electrolyte, the chemical dissolution of TiO_2 due to the presence of fluorine ion dominated over other two processes; the anodization process reached equilibrium in a very short time, and therefore, the film thickness was limited. It was found that, only within a certain anodization potential range, ordered TiO_2 nanotube arrays were formed.[3] In the present study, the effects of both electrolyte temperature and the anodization potential (especially at high voltage) on the formation of TiO_2 nanotube arrays were investigated. Figure 1 shows surface topologies of TiO_2 nanotube arrays obtained by anodizing 0.25 mm thick Ti foil in 0.5 wt % hydrofluoric acid at room temperature (Figure 1a) and in an ice bath (Figure 1b) for 1 h. The anodization was performed at 20 V. The nanotubes formed at room temperature had an average inner diameter of 50 nm and outer diameter of 110 nm, while the nanotubes obtained in the ice bath possessed an average inner diameter of 60 nm and outer diameter of 110 nm. At both anodization temperatures, there was slight difference in the inner diameter while the outer diameter was same. This observation may be because, at room temperature, the TiO_2 formation rate was higher than that in the ice bath, while the etching of TiO_2 induced by electric field and fluorine ion remained similar at both temperatures.

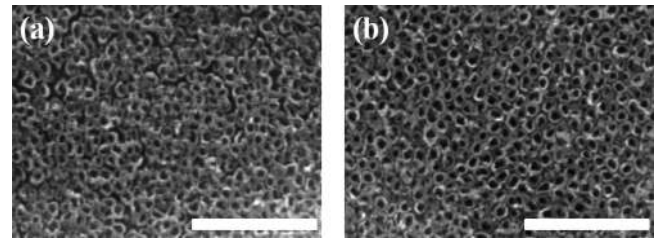

Figure 1. SEM topology of TiO_2 nanotube arrays obtained by anodization in 0.5 wt % hydrofluoric acid at 20 V anodization potential (a) at room temperature and (b) in an ice bath. Scale bar = 1 μm in both images.

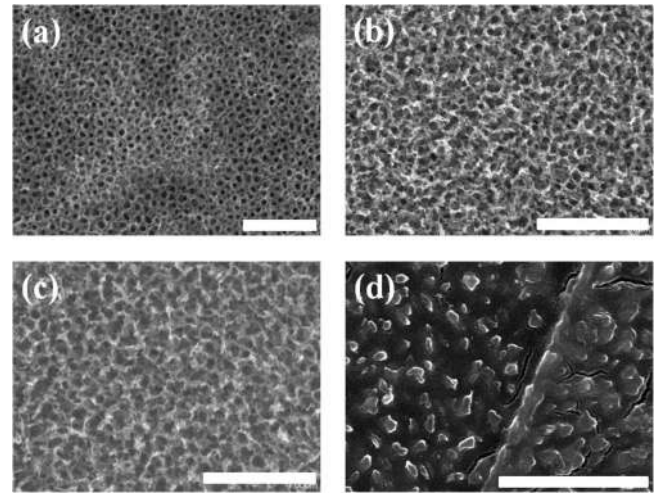

Figure 2. SEM topology of Ti foil anodized in 0.5 wt % hydrofluoric acid in an ice bath at various anodization potentials: (a) 20 V, (b) 60 V, (c) 80 V, and (d) 100 V. Scale bar = 1 μm in all images.

It has been reported that a certain anodization potential is necessary to yield ordered TiO_2 nanotube arrays, and 10 V was suggested as the lowest required potential.[3] In this study, we applied much higher anodization potential with the expectation of control over nanotube size. The surface topologies of Ti foil anodized at different potentials, that is, 20, 60, 80, and 100 V for 1 h, are shown in Figure 2. The anodization was conducted in an ice bath. As evidenced in the SEM images, at elevated anodization potential, that is, 60 and 80 V, the anodized Ti foil did not exhibit nanotubular structures; instead, a spongelike TiO_2 film with nanoholes was formed on the surface (Figure 2b and c). The formation of nanosponges instead of nanotubes may be due to the largely enhanced electrical field induced etching of TiO_2 at elevated anodization potential, although the electrochemical oxidation speed was also increased at higher anodization potential. The TiO_2 nanotubes formed by electrochemical oxidation of Ti were dissolved by both the chemical etching and the *enhanced* electrical field induced etching of TiO_2, resulting in the spongelike thin film of ~100 nm based on cross-sectional SEM imaging (data not shown). As the anodization potential was further increased to 100 V, only a dense film of

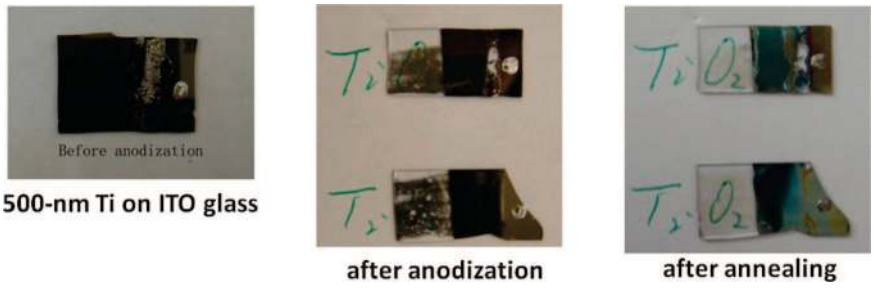

Figure 3. Digital images of Ti coated ITO glass before anodization (left panel), after anodization (center panel), and after thermal annealing (right panel).

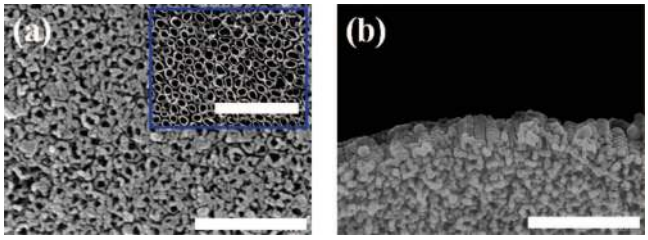

Figure 4. SEM images of electrochemically anodized Ti coated ITO glass. (a) Surface topology; inset shows the topology of 0.25 mm Ti foil electrochemically anodized under the same condition as the Ti coated ITO glass. (b) Cross section of the Ti thin film on ITO glass after anodization. Scale bar = 500 nm in all images.

TiO_2 was seen on top of the Ti foil (Figure 2d), which can be attributed to the even faster etching speed of TiO_2; that is, the formed TiO_2 via electrochemical oxidation was dissolved immediately in the electrolyte.

To demonstrate the flexibility of electrochemical anodization of Ti, rather than Ti foil, the Ti coated ITO glass was employed to grow TiO_2 nanotube arrays directly on the ITO glass surface. The ability to produce TiO_2 nanotube arrays on transparent substrates other than Ti foil renders semiconductor TiO_2 nanotubes for various applications, for example, DSSCs in a front-side illumination mode.[6] The use of TiO_2 nanotube arrays grown on fluorine-doped tin oxide (FTO) glass for DSSCs was reported to yield a power conversion efficiency of 2.9% with a film thickness of only 360 nm;[6] this is due to increased incident light harvesting efficiency as compared to the TiO_2 film grown on Ti foil, where the incident light was lost when passing through the top electrode and electrolyte.[4,5] In the present study, a 500 nm thick Ti film was deposited on cleaned ITO glass using an e-beam evaporator, followed by electrochemical anodization in 0.5 wt % hydrofluoric acid aqueous electrolyte (acetic acid was added with a volume ratio of 1:7). The anodization was performed in an ice bath at 12 V. Digital images in Figure 3 clearly show the change of Ti coated ITO glass before anodization, after anodization, and after subsequent thermal annealing. Initially, the Ti coated glass was dark. After anodization, the anodized area became semitransparent; upon subsequent thermal annealing at 500 °C, the anodized area changed to be optically transparent. Figure 4 shows the SEM images of TiO_2 nanotube arrays formed on ITO glass. Compared to the Ti foil anodized under the same conditions (inset in Figure 4a), the nanotube arrays formed on the ITO glass were less ordered and had thicker tube walls. This can be attributed to the short anodization time, which was limited by the original Ti film thickness predeposited. With a short anodization time, the self-organization process was not complete, leading to less ordered nanotube arrays. It is important to note that the quality of Ti films is critical to obtain highly ordered TiO_2 nanotube arrays,[6,22] and the quality of Ti thin films prepared by e-beam evaporation in the present study may not be as high as those deposited by radio frequency sputtering at high temperature.[6] Nonetheless, the TiO_2 nanotube arrays showed an average inner diameter of 30 nm and film thickness of 300 nm (Figure 4).

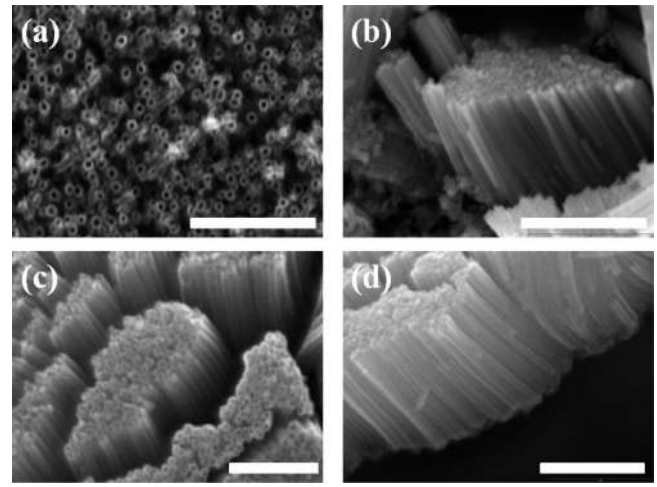

Figure 5. SEM images of TiO_2 nanotube arrays obtained by anodizing Ti foil in glycerol electrolyte at 40 V at (a, b) room temperature, scale bar = 2 μm for (a) and 5 μm for (b); (c, d) in an ice bath, scale bar = 500 nm for (c) and 1 μm for (d).

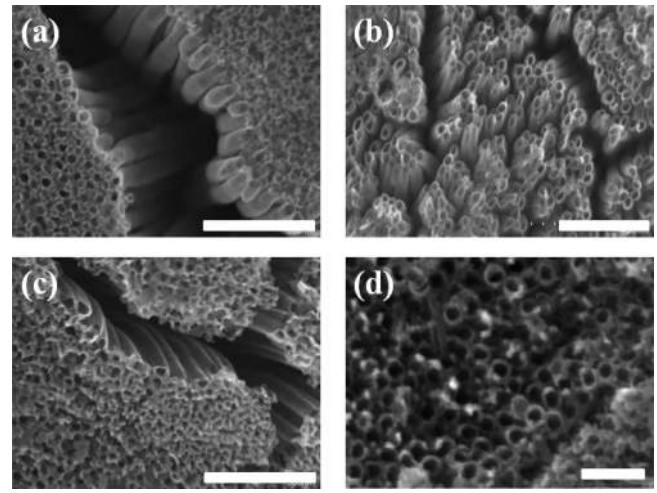

Figure 6. SEM images of Ti foil anodized at different anodization potentials. Glycerol electrolyte was used (0.25 wt % ammonium fluoride), and the anodizations were carried out in an ice bath at (a) 20 V, inner tube diameter = 20 nm; (b) 40 V, inner tube diameter = 20 nm; (c) 80 V, inner tube diameter = 25 nm; and (d) 100 V, inner tube diameter = 40 nm. Scale bar = 300 nm in all images.

2. TiO_2 Nanotube Arrays Obtained from Nonaqueous Electrolyte. Nonaqueous electrolytes (e.g., glycerol, ethylene glycol, etc.) containing fluorine ion have been used to fabricate highly ordered TiO_2 nanotube arrays with significantly increased

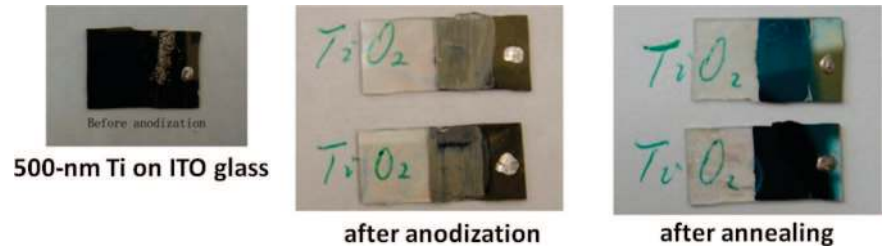

Figure 7. Digital images of 500 nm thick Ti coated ITO glass before anodization (left panel), after anodization (center panel), and after thermal annealing (right panel).

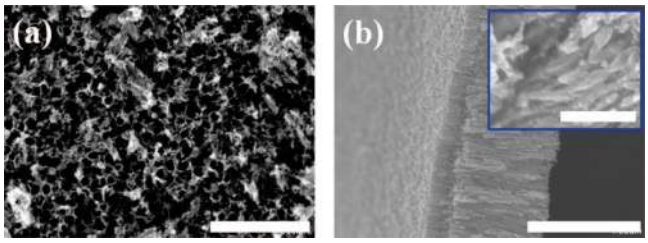

Figure 8. SEM images of Ti coated ITO glass anodized in glycerol at 60 V at at room temperature. (a) Surface topology, scale bar = 500 nm. (b) Cross-sectional view, scale bar = 1 μm; a closeup of the cross section is shown in the inset, scale bar = 250 nm.

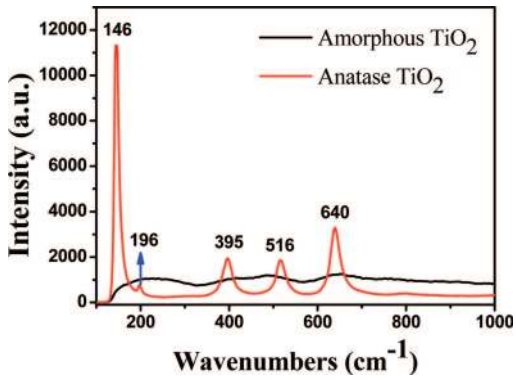

Figure 9. Raman spectra of the amorphous and annealed TiO_2 nanotube arrays. The spectra were obtained using an Ar laser with 5 mW intensity and 10 s acquisition time. The amorphous TiO_2 showed a broad spectrum, while the annealed TiO_2 exhibited specific peaks at 146, 196, 395, 516, and 640 cm^{-1}, which can be attributed to anatase TiO_2.

film thickness (e.g., nanotubes more than 100 μm in length have been successfully achieved[14,16,17]). This is because, in the nonaqueous electrolyte, the mobility of the fluorine ion was largely suppressed; thus, the chemical dissolution of TiO_2 was reduced. Similar to the anodization of Ti in aqueous electrolyte, we investigated the effect of electrolyte temperature and anodization potential using a nonaqueous electrolyte, namely, glycerol containing a small amount of ammonium fluoride. Ti foil with a thickness of 0.25 mm and 500 nm Ti coated ITO glass were anodized in the nonaqueous electrolyte. Figure 5 shows the SEM images of Ti foil anodized in glycerol containing 0.25 wt % ammonium fluoride at 40 V. The anodization was carried out either at room temperature (Figure 5a and b) or in an ice bath (Figure 5c and d). In both cases, highly ordered TiO_2 nanotube arrays with regular pore size and smooth tube walls were achieved, and the film thickness was several micrometers (e.g., a 5.5 μm thick film was obtained after 12 h anodization at room temperature). The TiO_2 nanotube arrays obtained at room temperature exhibited an average inner diameter of 90 nm and outer diameter of 110 nm (Figure 5a), and the regularity of nanotubes was much better than those produced in an aqueous electrolyte (Figure 1). When anodizing in an ice bath, the nanotube size was found to be largely reduced, having an average inner diameter of 20 nm and outer diameter of 50 nm (Figure 5c). When comparing with TiO_2 nanotubes obtained in aqueous electrolyte (i.e., hydrofluoric acid) where only a margin difference in nanotube diameter was observed (Figure 1a vs b), it was found that, in nonaqueous electrolyte (i.e., glycerol), the nanotube diameter was markedly affected by the electrolyte temperature (Figure 5a vs c). This can be understood as follows. At lower temperature (i.e., in the ice bath), the fluorine ion mobility in the viscous glycerol electrolyte was further suppressed, resulting in much slower etching of formed TiO_2, which in turn led to a smaller nanotube diameter. To the best of our knowledge, this is the first report on the effect of electrolyte temperature in the anodic formation of TiO_2 nanotube arrays.

When performing anodization in the ice bath, different anodization potentials ranging from 20 to 100 V were applied. At all applied potentials, highly ordered TiO_2 nanotube arrays were yielded, while the nanotube inner diameter did not change much. The SEM images of Ti foil anodized at different potentials in glycerol electrolyte (0.25 wt % ammonium fluoride) are shown in Figure 6. At 20 V, the nanotubes had an average inner diameter of 20 nm, yet not uniform along the nanotubes (Figure 6a); this is because, during the anodization, the current was so low (less than 1 mA) that the anodization potential automatically increased in order to continue the anodization (i.e., increased to 30 V after 2 h anodization as compared to the originally applied 20 V). With increased anodization potential, TiO_2 nanotube arrays with slightly increased inner diameter were obtained (i.e., 25 nm at 80 V and 40 nm at 100 V), indicating that although the anodization potential was increased, the chemical etching of TiO_2 by fluorine ion was still very low in the viscous electrolyte at low temperature; therefore, only a small difference in nanotube diameter was observed.

By anodizing Ti coated ITO glass in nonaqueous electrolyte (i.e., glycerol), rather than nanotube arrays, a nanoporous TiO_2 film was obtained. Digital images of Ti coated ITO glass before anodization, after anodization, and after subsequent thermal annealing are shown in Figure 7. Unlike the semitransparent film observed in aqueous electrolyte (hydrofluoric acid) (center panel in Figure 3), a completely transparent film on ITO glass was seen after anodizing in nonaqueous electrolyte (glycerol). Figure 8 shows the SEM images of the Ti coated ITO glass anodized in glycerol at 60 V at room temperature. A 1 μm thick nanoporous film was grown from the 500 nm predeposited Ti (Figure 8b). The formation of nanoporous films may be due to a combination of the reduced etching speed of TiO_2 in nonaqueous electrolyte and the incomplete self-organization process as a result of short anodization time (i.e., due to limited Ti film thickness). The increased film thickness (i.e., from original 500 nm Ti to 1 μm TiO_2) could be a result of both reduced etching of TiO_2 and volume expansion due to the

conversion from metallic Ti to porous TiO_2 upon anodization. The obtained nanoporous film had an average pore diameter of 35 nm as evidenced in the SEM image (Figure 8a).

3. Crystalline Formation in TiO_2 Nanotube Arrays. The TiO_2 nanotube arrays obtained directly after anodization were amorphous. In order to capitalize on them for applications in DSSCs, hydrogen generation, and so on, the amorphous TiO_2 should be transformed into crystalline anatase or rutile phase. Thus, thermal annealing on all anodized Ti (both foil and thin film on ITO) was performed at 500 °C in air for 3 h. The crystalline formation in the annealed TiO_2 nanotube arrays was confirmed by Raman scattering (Figure 9). The amorphous TiO_2 showed a broad spectrum (black curve in Figure 9), while the annealed TiO_2 exhibited specific peaks at 146, 196, 395, 516, and 640 cm^{-1} (red curve in Figure 9), which are signatures of the anatase TiO_2.[17] SEM imaging revealed that the TiO_2 nanotube arrays retained their nanotubular morphology despite high temperature thermal annealing (images not shown). It is worth noting that the TiO_2 nanotube arrays grown on ITO glass exhibited good transparency after thermal annealing (Figures 3 and 7), which is in good agreement with the results reported in the literature.[22]

Conclusions

In summary, high purity Ti foil and Ti thin film coated ITO glass were electrochemically anodized. The effects of electrolyte temperature and anodization potential on the formation of TiO_2 nanotube arrays were studied in both aqueous and nonaqueous electrolytes. In aqueous electrolyte, the anodization potential exerted significant influence on the formation of highly ordered TiO_2 nanotube arrays, while little effect from the electrolyte temperature was observed. In nonaqueous electrolyte, the electrolyte temperature markedly affected the TiO_2 nanotube dimensions, while, unlike in the aqueous electrolyte, anodization potential exhibited slight influence in this regard. With control over electrolyte temperature and anodization potential, highly ordered TiO_2 nanotube arrays with tube diameters ranging from 20 to 90 nm and film thicknesses ranging from several hundred nanometers to several micrometers can be readily obtained. To the best of our knowledge, this is the first report on the effect of electrolyte temperature. The TiO_2 nanostructures were examined by SEM. High temperature annealing of as-prepared TiO_2 nanotube arrays induced the formation of the anatase phase, which was confirmed by Raman scattering measurements.

Acknowledgment. This work was supported by a 3M Nontenured Faculty Award. J.W. thanks the Institute for Physical Research and Technology (IPRT) of Iowa State University for a Catron Fellowship. Scanning electron microscopy (SEM) was carried out at the Microscopy and Nanoimaging Facility (MNIF) at Iowa State University.

References and Notes

(1) Zwilling, V.; Darque-Ceretti, E.; Boutry-Forveille, A.; David, D.; Perrin, M. Y.; Aucouturier, M. *Surf. Interface Anal.* **1999**, *27*, 629.
(2) Zwilling, V.; Aucouturier, M.; Darque-Ceretti, E. *Electrochim. Acta* **1999**, *45*, 921.
(3) Gong, D.; Grimes, C. A.; Varghese, O. K.; Hu, W.; Singh, R. S.; Chen, Z.; Dickey, E. C. *J. Mater. Res.* **2001**, *16*, 3331.
(4) Paulose, M.; Shankar, K.; Varghese, O. K.; Mor, G. K.; Grimes, C. A. *J. Phys. D: Appl. Phys.* **2006**, *39*, 2498.
(5) Paulose, M.; Shankar, K.; Varghese, O. K.; Mor, G. K.; Hardin, B.; Grimes, C. A. *Nanotechnology* **2006**, *17*, 1446.
(6) Mor, G. K.; Shankar, K.; Paulose, M.; Varghese, O. K.; Grimes, C. A. *Nano Lett.* **2006**, *6*, 215.
(7) Zhu, K.; Neale, N. R.; Miedaner, A.; Frank, A. J. *Nano Lett.* **2007**, *7*, 69.
(8) Kongkanand, A.; Tvrdy, K.; Takechi, K.; Kuno, M.; Kamat, P. V. *J. Am. Chem. Soc.* **2008**, *130*, 4007.
(9) Wang, J.; Xu, J.; Goodman, M. D.; Chen, Y.; Cai, M.; Shinar, J.; Lin, Z. Q. *J. Mater. Chem.* **2008**, *18*, 3270.
(10) Varghese, O. K.; Gong, D.; Paulose, M.; Ong, K. G.; Dickey, E. C.; Grimes, C. A. *Adv. Mater.* **2003**, *15*, 624.
(11) Mor, G. K.; Varghese, O. K.; Paulose, M.; Ong, K. G.; Grimes, C. A. *Thin Solid Films* **2006**, *496*, 7.
(12) Varghese, O. K.; Gong, D.; Paulose, M.; Ong, K. G.; Grimes, C. A. *Sens. Actuators, B* **2003**, *93*, 338.
(13) Mor, G. K.; Shankar, K.; Paulose, M.; Varghese, O. K.; Grimes, C. A. *Nano Lett.* **2005**, *5*, 191.
(14) Shankar, K.; Mor, G. K.; Prakasam, H. E.; Yoriya, S.; Paulose, M.; Varghese, O. K.; Grimes, C. A. *Nanotechnology* **2007**, *18*, 065707.
(15) Mor, G. K.; Varghese, O. K.; Paulose, M.; Shankar, K.; Grimes, C. A. *Sol. Energy Mater. Sol. Cells* **2006**, *90*, 2011.
(16) Prakasam, H. E.; Shankar, K.; Paulose, M.; Varghese, O. K.; Grimes, C. A. *J. Phys. Chem. C* **2007**, *111*, 7235.
(17) Wang, J.; Lin, Z. Q. *Chem. Mater.* **2008**, *20*, 1257.
(18) Macak, J. M.; Tsuchiya, H.; Schmuki, P. *Angew. Chem., Int. Ed.* **2005**, *44*, 2100.
(19) Macak, J. M.; Tsuchiya, H.; Taveira, L.; Aldabergerova, S.; Schmuki, P. *Angew. Chem., Int. Ed.* **2005**, *44*, 7463.
(20) Paulose, M.; Shankar, K.; Yoriya, S.; Prakasam, H. E.; Varghese, O. K.; Mor, G. K.; Latempa, T. A.; Fitzgerald, A.; Grimes, C. A. *J. Phys. Chem. B* **2006**, *110*, 16179.
(21) Albu, S. P.; Ghicov, A.; Macak, J. M.; Hahn, R.; Schmuki, P. *Nano Lett.* **2007**, *7*, 1286.
(22) Mor, G. K.; Varghese, O. K.; Paulose, M.; Grimes, C. A. *Adv. Funct. Mater.* **2005**, *15*, 1291.
(23) Macak, J. M.; Tsuchiya, H.; Berger, S.; Bauer, S.; Fujimoto, S.; Schmuki, P. *Chem. Phys. Lett.* **2006**, *428*, 421.
(24) Sadek, A. Z.; Zheng, H.; Latham, K.; Wlodarski, W.; Kalantar-zadeh, K. *Langmuir* **2009**, *25*, 509.
(25) Varghese, O. K.; Gong, D.; Paulose, M.; Grimes, C. A.; Dickey, E. C. *J. Mater. Res.* **2003**, *18*, 156.

JP811201X